TECHNICAL ADVANCE

Parallel recordings of photosynthetic electron transport and K$^+$-channel activity in single guard cells

Chang-Hyo Goh[1,2], Petra Dietrich[1], Ralf Steinmeyer[1], Ulrich Schreiber[1], Hong-Gil Nam[1] and Rainer Hedrich[1,*]

[1]*Julius-von-Sachs Institut für Biowissenschaften, Lehrstuhl für Molekulare Pflanzenphysiologie und Biophysik, Julius-von-Sachs-Platz 2, 97082 Würzburg, Germany, and*
[2]*Division of Molecular and Life Science, Pohang University of Science and Technology, Pohang 790-784, Korea*

Summary

Stomata open in response to red and blue light. Red light-induced stomatal movement is mediated by guard cell chloroplasts and related to K$^+$-uptake into these motor cells. We have combined a new type of microchlorophyll fluorometer with the patch–clamp technique for parallel studies of the photosynthetic electron transport and activity of plasma membrane K$^+$ channels in single guard cell protoplast. In the whole-cell configuration and presence of ATP in the patch-pipette, the activity of the K$^+$-uptake channels remained constant throughout the course of an experiment (up to 30 min) while photosynthetic activity declined to about 50%. In the absence of ATP inward K$^+$ currents declined in a time-dependent manner. Under these ATP-free conditions, photosynthetic electron transport was completely blocked within 8 min. ADP together with *ortho*phosphate was able to prevent inhibition of photosynthetic electron transport and run-down of K$^+$-channel activity. The results demonstrate that the combination of these two techniques is suited to directly study cytosolic factors as common regulators of photosynthesis and plasma membrane transport within a single-cell.

Key words: ATP, chlorophyll fluorescence, electron transport, guard cell, K$^+$ channel, patch–clamp.

Introduction

Light-dependent stomatal opening requires activation of the H$^+$-pump, which hyperpolarizes the membrane and acidifies the apoplast (Blatt, 1988; Felle *et al.*, 2000; Lohse and Hedrich, 1992; Roelfsema *et al.*, 2001). When Serrano *et al.* (1988) blocked photosynthetic electron transport of guard cells by DCMU in the presence of saturating concentrations of ATP red light-induced H$^+$ pumping diminished. In these experiments, ADP and Pi could partially replace ATP to fuel the H$^+$-pump. Upon supplementation of cytosolic ATP with *ortho*phosphate, red light-stimulated pumping increased, although *ortho*phosphate does not stimulate the H$^+$-ATPase *in vitro*. It was, therefore, concluded that ATP and additional chloroplast-derived factors account for the red-light effect (Serrano *et al.*, 1988).

Besides the H$^+$-ATPase, which requires MgATP to power H$^+$ transport, ATP-sensitive K$^+$ channels have been identified in guard cells (Wu and Assmann, 1995). Likewise, the guard cell K$^+$-channels *KST1* and *KAT1* after heterologous expression in *Xenopus* oocytes exhibit a pronounced ATP-dependence (Hoshi, 1995; Müller-Röber *et al.*, 1995). In this context, it should be noted that illuminated chloroplasts of mesophyll cells produce a factor, which acts on the plasma membrane potential (Spalding and Goldsmith, 1993). Using plasma membrane patches, the authors could show, that ATP stimulates K$^+$ channels in the plasma membrane. This provides indirect evidence for the activation of plasma membrane K$^+$ channels by ATP produced photosynthetically.

While photosynthesis in mesophyll cells has been extensively studied, its precise role for stomatal opening is still under debate. This was, at least in part, due to the difficulty of obtaining reliable quantitative information on photosynthetic reactions of guard cells. These limitations, however, have been overcome by the introduction of a

microchlorophyll fluorometer (Schreiber, 1998), which allows the assessment of photosynthetic electron transport using the saturation pulse method (Schreiber *et al.*, 1994). Goh *et al.* (1999) applied this technique to study the photosynthetic properties of intact guard cells and single guard cell protoplasts in detail. An important outcome of this work was the finding that photosynthetic electron transport in guard cells is severely suppressed under anaerobiosis and in the presence of fusicoccin. The loss of electron flow, could be prevented by blocking ATP consumption of the plasma membrane ATPase or by glucose addition, which stimulates ATP formation by mitochondrial respiration.

In order to study the effect of cytosolic ATP on both nucleotide-dependent systems, photosynthesis and plasma membrane ion channels simultaneously, we combined two single-cell techniques: the MICROSCOPY-PAM fluorescence analysis and the patch–clamp technique. 'Patch-pipette biochemistry' in the whole-cell configuration enabled us to manipulate the composition of the cytosol. Experiments in the presence and absence of cytosolic ATP revealed that the activity of plasma membrane K$^+$-uptake channels as well as the photosynthetic electron transport of the guard cell chloroplasts depends on the presence of ATP. Besides providing evidence for cytosolic nucleotides as important regulator of photosynthesis and ion channel activity the results demonstrate that the combination of the two single-cell techniques is suited to directly study the role of common cytosolic factors on both processes.

Results

Patch–clamp and chlorophyll fluorescence recordings on the same guard cell protoplast

To explore the ATP-dependence of guard cell photosynthesis and the plasma membrane K$^+$ channels, we used single guard cell protoplasts from *Vicia faba* leaves and applied two single-cell techniques, the patch–clamp technique (Hamill *et al.*, 1981) and the MICROSCOPY-PAM chlorophyll fluorescence analysis (Goh *et al.*, 1999). Patch-pipettes were attached to protoplasts containing intact chloroplasts and exhibiting cytoplasmic streaming as a viability marker. After tight seals were formed between the pipette and the plasma membrane, we established the whole-cell configuration, a micropipette-cytoplasm continuum, by rupturing the membrane patch underlying the pipette tip through a short suction pulse. The resulting whole-cell configuration was characterised by a mean access resistance of $R_s = 19.53 \pm 8.6 \, M\Omega$ and a membrane capacitance of $C_m = 9.20 \pm 1.0 \, pF$ ($n = 41$).

With the establishment of the whole-cell configuration the diffusion of various molecular components from the pipette into the cytosol and *vice versa* is initiated. As a

result, many cell properties and functions are likely to be modified or even severely disturbed. We, therefore, monitored two independent processes in two different membrane systems within individual guard cells, photosynthetic electron transport in the thylakoid and K$^+$ transport across the plasma membrane in response to changes in the nucleotide supply.

Photosynthetic electron transport

Figure 1 shows recordings of dark–light induction kinetics of single guard cell protoplasts in the presence and absence of ATP in the patch-pipette. Measurements right after establishment of the whole-cell configuration (0.5 min) and after
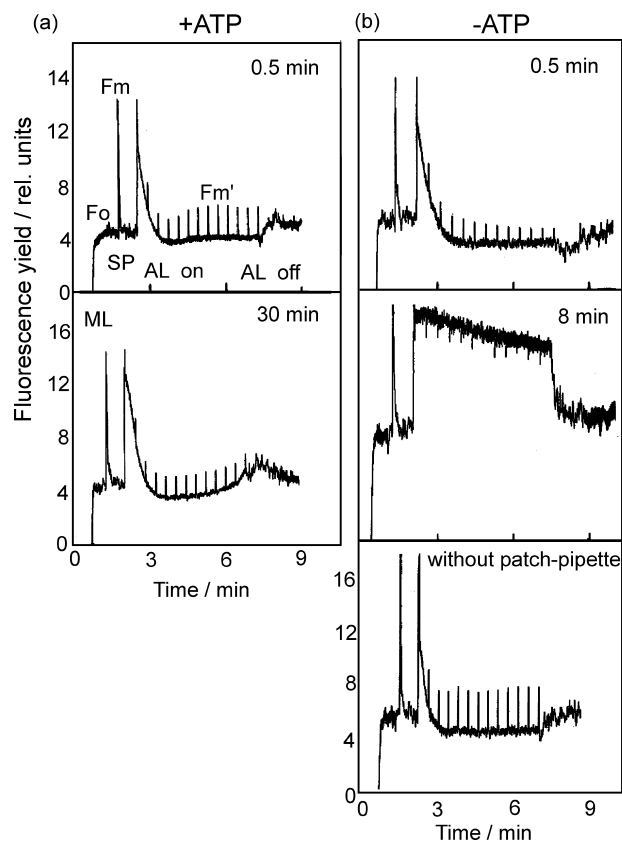

Figure 1. Inhibition of photosynthetic electron transport in *V. faba* guard cell protoplasts upon depletion of ATP in the whole-cell configuration. Recordings of dark–light induction transients of single guard cell protoplasts in the whole-cell configuration with fluorescence-quenching analysis by the saturation pulse method. Measuring light (ML) intensity was 0.8 μmol m^{-2} sec^{-1} of photosynthetically active radiation. Saturation light pulses (SP) inducing maximal fluorescence yields were applied at 40 sec following onset of ML and every 30 sec after onset of actinic light (AL).
(a) Presence of 2 mM MgATP in the standard patch-pipette solution at 0.5 min (upper graph) and 30 min (lower graph) after establishment of the whole-cell configuration.
(b) Absence of MgATP in the standard patch-pipette solution at 0.5 min (upper graph) and 8 min (middle graph) after establishment of the whole-cell configuration. Recording of a 'non-patched' protoplast adjacent to that investigated in the upper and middle panel shows normal photosynthetic electron transport (lower graph).

equilibration of the pipette solution with the cytosol (8–30 min) are presented. For comparison also a measurement on a patch-pipette-free protoplast is shown. Each measurement involves assessment of the minimal fluorescence yield (F_o) of the dark-adapted sample, determination of maximal fluorescence yield (F_m) by application of a saturation pulse to the dark-adapted sample and recording of the fluorescence change upon onset of actinic illumination, with repetitive determination of the maximal fluorescence yield ($F_{m'}$) by saturation pulses at 30 sec intervals. The relative fluorescence increase induced by a saturation pulse ($\Delta F/F_m$ or $\Delta F/F_{m'}$) represents the Photosystem II (PS II) quantum yield (Y) and, hence, at a given photon flux density may serve as a measure of photosynthetic electron transport rate (Genty *et al.*, 1989; Schreiber *et al.*, 1994). Without going into details about complex induction kinetics, two major findings are apparent from the data of Figure 1. First, when ATP was absent from the patch-pipette, already 8 min after establishment of the whole cell configuration the quantum yield of charge separation at PS II declined to zero upon application of actinic light ($Y=0.00$). Actually, in this situation saturation pulses induced negative fluorescence changes, likely to be caused by transient accumulation of reduced pheophytin, indicative of an extreme block of the PS II acceptor side (Klimov *et al.*, 1977). Second, when ATP was present in the patch-pipette inhibition of electron transport was less pronounced. This time-dependent lowering of the electron transport rate most likely resulted from equilibration of the cytoplasm with the pipette solution during whole-cell measurements. While 0.5 min after establishment of whole-cell configuration the effective quantum yield was only slightly lower than in the absence of a patch–pipette ($Y=0.37$ with respect to 0.39), after 30 min electron transport rate was cut almost to half ($Y=0.20$).

These data show that our microfluorescence single-cell technique allows distinguishing between the dramatic inhibition of photosynthetic electron transport caused by ATP depletion and the slower 'run-down' following the establishment of the whole-cell configuration. Based on these initial result, two questions arise: First, what causes the 'run-down process' in the presence of ATP and second, how does ATP depletion affect photosynthesis? The run-down of photosynthetic electron transport during whole-cell measurements points to the requirement for supplementation of our very basic cytoplasmic solution, containing 2 mM ATP and 150 mM K$^+$ buffered to nanomolar Ca^{2+} concentrations, only (see paragraph on diffusion below). Regarding the dramatic decline of photosynthetic activity upon ATP depletion, the presented data confirm previous conclusions by Goh *et al.* (1999). Phenomenologically, the dark–light induction kinetics in the absence of ATP are identical to those previously observed in the presence of fusicoccin and under anaerobiosis. In both cases, a depletion of ATP had been suggested, as fusicoccin stimulates

massive ATP consumption by the plasma membrane H$^+$-ATPase and anaerobiosis suppresses oxidative phosphorylation in the mitochondria (Goh *et al.*, 1999). As a neighbouring protoplast without patch-pipette did not display symptoms of inhibition (bottom trace of Figure 1b), it appears unlikely that protoplasts in the measuring chamber generally suffered from anaerobiosis. ATP depletion of the cytosol might, therefore, stimulate mitochondrial O$_2$ uptake to an extent that local symptoms of anaerobiosis could develop. To decide whether local O$_2$-depletion develops during whole-cell measurements, cytoplasmic O$_2$ measurements with a high spatial resolution have to be established.

K$^+$-channel activity

Previous studies provided evidence for voltage-dependent K$^+$-uptake channels in the plasma membrane of guard cells to represent an ATP-dependent membrane protein (Hoshi, 1995; Müller-Röber *et al.*, 1995; Wu and Assmann, 1995). In the presence of ATP in the patch-pipette this channel activates with slow kinetics whenever the membrane potential is more negative than about −80 mV. This behaviour, well known from previous studies (Schroeder *et al.*, 1987; Schroeder, 1988) remained unchanged even for prolonged times, when exposed to ATP supplied via the patch-pipette (16 min in Figure 2a). Using ATP-free pipette solutions inward K$^+$ currents after 16 min represent only 40% of the current recorded right after whole-cell access (Figure 2b).
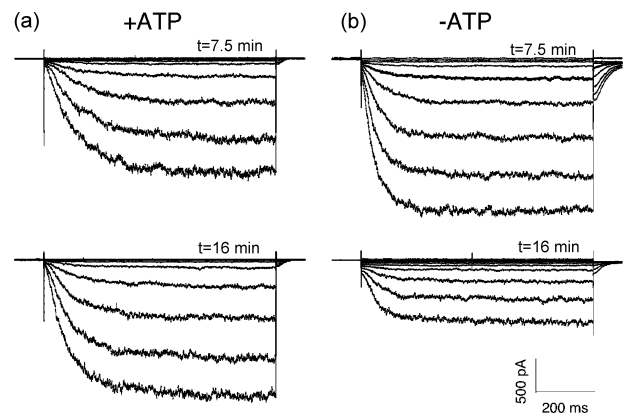

Figure 2. Plasma membrane K$^+$-inward currents depend on cytosolic ATP. Using the same protoplasts as for the fluorescence measurements of Figure 1. K$^+$ inward currents were elicited by 800 ms pulses to voltages between −36 and −216 mV in 20 mV-decrements starting from a holding potential of −56 mV.

(a) Inward K$^+$-channel activity was recorded in the presence of 2 mM MgATP in the standard pipette solution (see Figure 1 and Experimental procedures). Similar responses were observed at 7.5 min (upper panel) and 16 min (lower panel) after whole-cell access. Holding potential after test pulses was −56 mV, $C_m = 10.0$ pF.

(b) Electrical recordings of K$^+$ currents were performed using an ATP-free pipette solution. Comparison of the K$^+$-current amplitudes at 7.5 min (upper panel) and 16 min (lower panel) after whole-cell access revealed a time-dependent decline. Holding potential after test pulses was −96 mV, $C_m = 10.1$ pF.

This run-down of K^+-channel activity in ATP-free solutions was observed in all guard cell protoplasts characterised by the emerging block of photosynthetic electron transport ($n = 22$). From the time-dependent recordings of corresponding K^+ current–voltage curves the mechanism of ATP depletion was explored (Figure 3). In ATP-containing solutions, the activation kinetics (Figure 3a, upper traces) as well as the overall current–voltage relations of the K^+-inward channel (Figure 3a, lower graph) remained stable during an experiment of 39 min duration. By contrast, ATP-depletion in the cytosol caused a pronounced decrease in K^+ currents within 30 min (Figure 3b). Re-scaling of the current at −196 mV after 15.5 min revealed, that activation kinetics was not significantly affected during ATP loss from the cytosol (grey curve in Figure 3b, upper graph). After normalisation of the decreasing current amplitudes in the absence of ATP (Figure 3b, open circles versus filled circles), similar current–voltage curves were obtained for all time points tested. It is, therefore, very likely, that ATP depletion acts via reduction of the number of voltage-sensitive K^+ channels in the plasma membrane rather than on the steady-state open probability. With KAT1 heterologeously expressed in *Xenopus* oocytes, however, ATP-depl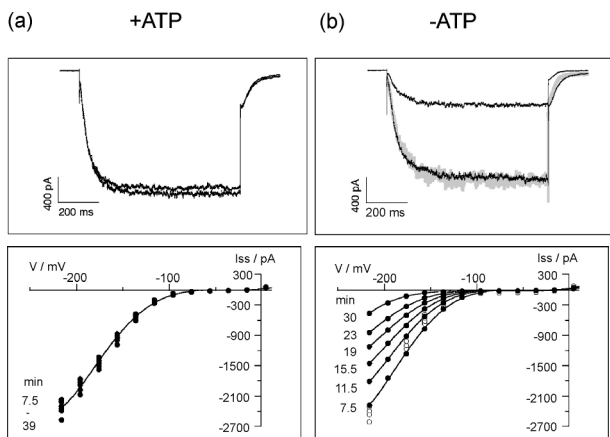etion experiments revealed a shift in the voltage-dependence as well (Hoshi, 1995). The former effect on the channel number, which was not observed with KAT1 homomers, may result from the heteromeric composition of K^+-channel α-subunits in guard cells (Szyroki *et al.*, 2001).

Is diffusional loss of ATP responsible for the run-down of photosynthesis and K^+-channel activity?

Low molecular weight solutes such as nucleotides and phosphate are lost from guard cells during whole-cell measurements. We thus tested, whether diffusion processes are responsible for the loss of K^+-channel activities and electron transport capacity of the chloroplasts. Exchange rates of solutes of various sizes within the guard cell-micropipette system were analysed with fluorescent probes of different molecular weights. For this purpose, patch-pipettes were filled with acridine orange (240 g mol^{-1}) and fluorescein-coupled dextranes (3000, 10 000 and 40 000 g mol^{-1}) and the time-dependent increase in guard cell-fluorescence was monitored. Figure 4(a) shows the increase in fluorescence due to the diffusion of acridine orange into the guard cell cytoplasm (0 and 100 sec after whole-cell formation). The equilibration process between the fluorochrome-containing pipette solution and the cell interior was characterised by a saturation-type of behaviour (Figure 4b). For modelling the diffusion process, the volume covered by the pipette tip and the guard cell was divided into cubes of $10^{-3}\ \mu m^3$ (Figure 4c). The dye flux into the guard cell was then fitted varying the diffusion constants in the model as described in Experimental procedures. The diffusion rates determined from the fluorescent measurements changed systematically with the molecular weight of the dye (Figure 4d). For the cells investigated, we found the time-constant τ for solute exchange to depend on the molecular weight M according to:

$$\tau = 8.8 \cdot M^{0.31} \qquad (1)$$

with τ in seconds and M in g mol^{-1}. From the calibration curve obtained with metabolically inactive compounds (Figure 4d; equation (1)), a time-constant of 70 sec was predicted for the loss of ATP (465 g mol^{-1}) from the cytoplasm into an ATP-free patch-pipette. This time constant is six times faster compared to the K^+-channel run-down in the absence of ATP from the pipette, which was characterised by a time-constant of 6.9 min (Figure 5, open circles). Given initial millimolar concentrations of ATP in the cytosol, the ATP concentration 10 min after whole-cell access would be in the micromolar range. Channel recruitment thus appears to involve at least one ATP-dependent process in the high-affinity range such as phosphorylation (Li *et al.*, 1998; Mori and Muto, 1997; Tang and Hoshi, 1999). Similar conclusions were drawn from whole-cell measurements in the presence of glucose in addition to

Figure 3. ATP prevents loss of K^+-channel activity.
(a) Upper graph: K^+-inward currents of one guard cell protoplast upon hyperpolarization to −196 mV at 7.5 and 24 min after whole cell access in the presence of 2 mM MgATP in the patch-pipette. Superposition of the current traces indicates the absence of channel run-down. Lower graph: steady-state current–voltage relation of K^+ channels from the same protoplast at 7.5, 12.5, 16.5, 20, 24 and 39 min after whole-cell access. $C_m = 10.2$ pF.
(b) Upper graph: K^+-inward currents of one guard cell protoplast upon hyperpolarization to −196 mV at 7.5 and 15.5 min after whole cell access in the absence of ATP. Normalising the current trace after 15.5 min to the steady-state current after 7.5 min revealed, that channel run-down was not due to changes in the activation kinetics (grey curve). Lower graph: steady-state current–voltage relation of K^+ channels from the same protoplast at 7.5, 11.5, 15.5, 19, 23 and 30 min after whole-cell access. Differences in current amplitudes are due to a time-dependent change in the number of active channels rather than their voltage dependence as seen from the rescaled data points (○). For re-scaling, the current voltage curves were normalised to the value at $t = 7.5$ min and $V = -196$ mV; $C_m = 9.9$ pF.

Figure 5. Effect of nucleotide composition of patch-pipette solution on time-dependent run-down of K+-channel activity.

Steady-state whole-cell K+ currents at -196 mV were normalised to the value at 7.5 min after whole-cell access and plotted against the measuring time. In the presence of ATP ($\bullet$, $n = 18$) or ADP in addition to *ortho*phosphate ($\diamondsuit$, $n = 11$) in the patch-pipette channel activity is maintained up to 30 min in the whole-cell configuration. Removal of ATP from the patch-pipette ($\bigcirc$, $n = 16$) induced a time-dependent channel run-down. Data points in the presence and absence of ATP were exponentially fitted (lines). For run-down of K+-channel activity a time constant of 6.9 min was determined. Data presented were obtained from the same protoplasts on which measurements of photosynthetic electron transport was performed (Figures 1 and 6).
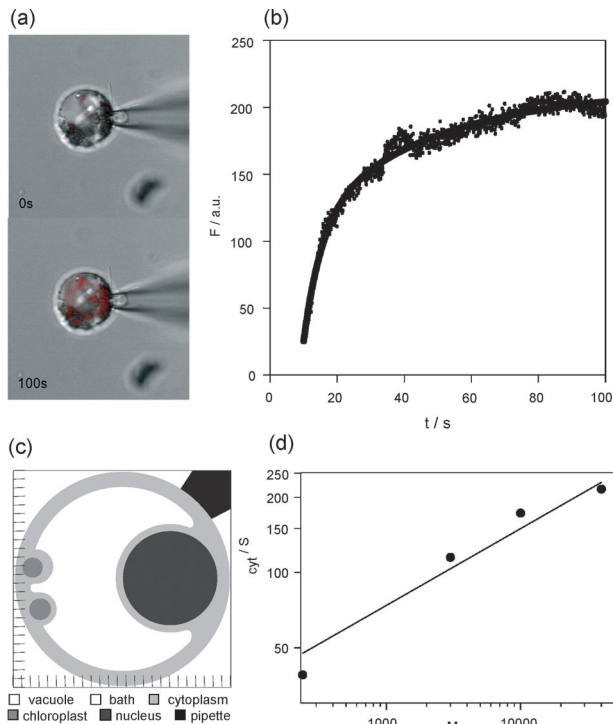

Figure 4. Diffusion model.

(a) Diffusion of acridine orange from a patch-pipette into a *V. faba* guard cell protoplast 0 and 100 sec after whole-cell access (red = fluorescence intensity at 515–565 nm, grey = microscopic image, $C_m = 9.0$ pF, $R_S = 11$ MΩ).

(b) Time course of the corresponding fluorescence intensity F in the cell (au = arbitrary units; dots = measured data points, line = modelled curve).

(c) One layer from the model of a protoplast. The depicted area is divided into small squares of different subcellular origin. The different grey-levels denote vacuole, bath, cytoplasm, chloroplasts, nucleus and pipette.

(d) Plot of diffusion time constants τ_{cyt} versus the molecular weight M of the dyes. Symbols represent measurements for acridine orange ($M = 238$ g mol^{-1}), and fluorescein coupled dextranes ($M = 3000$, $10\,000$, $40\,000$ g mol^{-1}). The straight line corresponds to a fit using the parameters from equation (1).

hexokinase, a treatment that reduced K+-channel currents by only 30–40% after 10 min (Wu and Assmann, 1995). Since ATP-dependent regulation of K+-channel activity has also been observed in inside-out membrane patches (Müller-Röber *et al.*, 1995; Wu and Assmann, 1995), high-affinity ATP-hydrolysis or binding is very likely to underlie this effect. The latter process has also been reported to account for deviations of diffusion constants for cyclic nucleotides from the diffusion model applied to chromaffin cells (Pusch and Neher, 1988).

ADP and orthophosphate prevent inhibition of photosynthetic electron transport and run-down of K+-channel activity

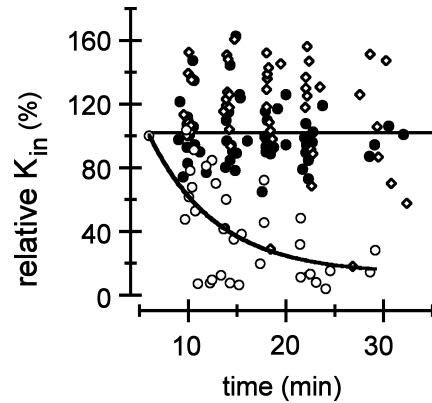Using ATP-free solutions, not only ATP but also ADP and *ortho*phosphate are likely to leak out from the cytosol into the patch-pipette, thereby becoming limiting for photosynthesis. We, therefore, tested whether addition of ADP and *ortho*phosphate can prevent the run-down of K+-channel activity and inhibition of photosynthesis. As shown in Figure 5, the run-down of K+ currents observed in the absence of ATP (open circles) was prevented over the course of the 30 min whole-cell measurements when ADP plus Pi was present (open rhombus), thus being indistinguishable from the situation in presence of ATP (filled circles).

As a measure for photosynthetic activity, we compared the fluorescence derived relative electron transport rates in the presence of ATP and ADP plus Pi (Figure 6) While no significant differences between these two treatments were observed immediately after whole-cell access (Figure 6a), 23 min later the electron transport rates in the presence of ADP plus Pi were significantly below those in the presence of the nucleotide-triphosphate (Figure 6b). It should be noted, however, that the presence of ADP plus Pi prevented the dramatic inhibition of photosynthetic electron transport observed in the absence of ATP (see Figure 1). Obviously, ATP-synthesis by mitochondria under these conditions was sufficient to compensate ATP loss via the patch-pipette. Together, these results demonstrate, that nucleotides and *ortho*phosphate represent limiting factors for photosynthesis in the absence of ATP. They furthermore show that this approach is suitable to study guard cell physiology and, in particular, the complex regulatory interactions between cytosol, chloroplasts, mitochondria and plasma membrane.
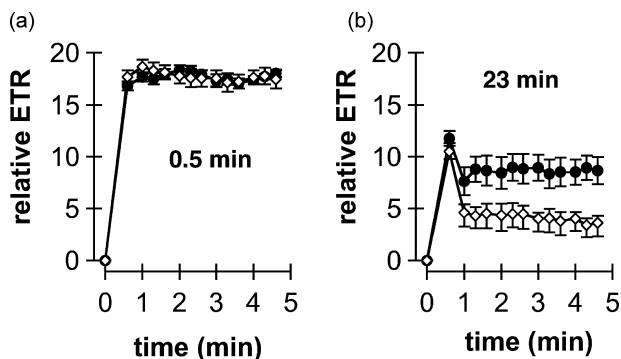
(a)

(b)

Figure 6. Effect of nucleotides on time-dependent decline of photosynthetic electron transport rate after establishment of whole-cell configuration. Corresponding K^+-channel activities from the same protoplasts are implemented in Figure 5.
(a) Relative electron transport rates (ETR) directly (0.5 min) after the establishment of the whole-cell configuration. Relative ETR values were calculated from the fluorescence parameters measured in the course of dark–light induction curves starting 0.5 min after whole-cell access, as shown in Figure 1. Pipette solutions contained either 2 mM ATP ($\bullet$, $n = 8$) or 2 mM ADP + 2 mM Pi ($\diamond$, $n = 8$). Data points represent mean values ± SEM.
(b) Relative electron transport rates (ETR) calculated from the fluorescence parameters measured in the course of dark–light induction curves starting 23 min after establishment of the whole-cell configuration. Presentation as in Figure 5; ATP ($n = 8$), ADP + Pi ($n = 7$).

Discussion

A recent analysis of the inhibition of photosynthetic electron transport in guard cell chloroplasts by fusicoccin and anaerobiosis revealed a central role of the cytoplasmic ATP pool and O_2 concentration in the control of chloroplast activity (Goh *et al.*, 1999). Our present study builds on the observation that the loss of photosynthetic activity in the presence of the fungal toxin fusicoccin is overcome by either blocking the ATP consuming H^+ pump, hyperactivated by binding the 14-3-3 protein (Sze *et al.*, 1999 and references therein), or glucose treatment. Besides altering the ATP content of the guard cell, anaerobiosis and fusicoccin may also affect the cytoplasmic pH and Ca^{2+} concentration (Bertl and Felle, 1985; Felle *et al.*, 1986). We, therefore applied, the whole-cell configuration of the patch–clamp technique to control the ATP concentration and to introduce pH- and Ca^{2+}-buffers into guard cell protoplasts. Patch-pipette solutions were designed to clamp the cytosolic Ca^{2+} to nanomolar levels and the pH to 7.4. When supplemented with 2 mM MgATP, the inward rectifier displayed a stable activity for up to 30 min, whereas photosynthetic activity declined to about 50%. In the absence of ATP, however, photosynthetic activity was completely suppressed and inward K^+ currents strongly declined. Since ADP, AMP, GTP, or the non-hydrolyzable AMP-PNP are unable to replace ATP for activation of K^+-uptake channels (Hoshi, 1995), inward K^+ currents represent an indicator for the presence of ATP in the cytosol.

ATP production and consumption in guard cells

During stomatal opening in the light starch is broken down and oxaloacetic acid is reduced to malate (Michalke and Schnabl, 1990). Apoplastic K^+ and Cl^- are taken up against their concentration gradient, and together with malate, accumulate in the vacuole (Raschke, 1979). These processes consume reduction equivalents and ATP, which are provided by photosynthesis and respiration. A crosstalk between guard cell chloroplasts and mitochondria has previously been shown (Gautier *et al.*, 1991; Mawson, 1993). Upon reduction of the oxygen concentration, photosynthesis and respiration, both decayed. This observation is in line with Goh *et al.* (Goh *et al.*, 1999) who documented that the loss of photosynthesis can be prevented by glucose feeding in a cyanide-sensitive manner. Low-oxygen concentrations may develop during the removal of ATP from the cytoplasm due to the stimulation of oxidative phosphorylation and ATP production in the mitochondria. By contrast, in the presence of ATP in the patch-pipette, the triosephosphate–*ortho*phosphate shuttle of the chloroplast inner envelope will initially export photosynthates generated by the Calvin cycle, but finally will run low of cytoplasmic *ortho*phosphate. A feedback on the dark and light reaction might explain the decrease in photosynthesis in the presence of ATP (Figures 1a and 6). Export of triosephosphates under low ATP-to-triosephosphate ratios is also promoted by an ion channel identified in the chloroplast outer envelope (Bölter *et al.*, 1999).

Conclusion

To our knowledge, this is the first report on parallel measurements of photosynthetic electron transport and ion channel activity in one and the same protoplast, the cytoplasmic composition of which was controlled by manipulation of the patch-pipette solution. The way is now open for a detailed study of the factors controlling guard cell physiology and the interaction between guard cell chloroplasts and plasma membrane ion channel activity. Upon establishment of the whole-cell configuration, there is a time-dependent decline of photosynthetic activity, the extent of which depends on the content of ATP and ADP plus Pi in the patch-pipette. Run-down of K^+-channel activity was only observed when ATP was omitted from the patch-pipette solution. Obviously, the ATP-requirement of K^+-channel activity is distinctly lower than that of photosynthetic electron transport. Regarding the mechanism of electron transport inhibition upon ATP-depletion, the well-known ATP-demand of photosynthetic CO_2 fixation does not provide a satisfactory explanation. From the pronounced O_2-dependence of electron transport revealed by fluorescence-quenching analysis during the first minute of dark–light induction it may be assumed that in the absence of ATP the

local O_2 concentration is too low to support O_2-dependent electron transport. Future approaches may thus aim to measure O_2 gradients within the guard cell cytoplasm with a high spatial resolution.

Experimental procedures

Plant material and protoplast isolation

Broad bean (*V. faba* L. cv. Grünkernige Hangdown, Gebag, Hannover, Germany) plants were grown in a greenhouse at 20–24°C/14–16°C (day/night) at a photon flux density of 300 µmol m^{-2} sec^{-1} and a light period of 14 h. Fully expanded leaves from the third to fourth nodes of 3–4-week-old plants were used in the experiments. Leaves were harvested between 09.00 and 09.30 am for all experiments. Protoplasts from guard cells and mesophyll cells were enzymatically isolated as previously described (Goh *et al.*, 1999).

Diffusion model

Diffusion measurements were performed in the tight seal whole-cell configuration of the patch–clamp technique (Hamill *et al.*, 1981). The increase of fluorescence of the guard cell protoplast was measured with a Zeiss laser scan microscope (LSM 410, Carl Zeiss GmbH, Göttingen, Germany) after rupturing the membrane between the fluorochrome-containing pipette and the cytosol. Acridine orange and fluorescein-labelled dextrans in the mole weight range between 240 and 40 000 g mol^{-1} were excited using a 488-nm argon laser. Fluorescence intensity was measured as the mean value obtained from the area covered by the cell.

Diffusion of dissolved substances follows Fick's law:

$$\frac{\partial c(\vec{r}, t)}{\partial c} = D(\vec{r})\Delta c(\vec{r}, t) \qquad (2)$$

where $c(\vec{r}, t)$ is the concentration at the location $\vec{r}$ and time t and $D(\vec{r})$ represents the diffusion constant at the location $\vec{r}$. This differential equation cannot be solved analytically for a complex geometry like the *V. faba* guard cell attached to a pipette in the whole cell configuration. We, therefore, developed a model with the space of the pipette and the protoplast divided into small cubes. For the latter, the individual cubes are either located in the cytoplasm, the vacuole, the nucleus or a chloroplast. The cubes are then characterised by their diffusion constants, which were zero for all dextran-coupled dyes in all compartments but the cytoplasm. Using this model equation (2) can be substituted by a set of difference equations:

where $c(x, y, z)$ is the concentration in the cube at position (x, y, z) and, e.g. $D_{x\pm1, y, z}$ the diffusion coefficient for the solute exchange between the cube (x, y, z) and $(x\pm1, y, z)$. Assuming that the concentration remains constant in the bath solution and in the pipette at ≥ 1 µm away from the cell this system (equation (3)) was solved numerically for each cube to follow the time course of concentration changes within each cube. At each measuring time, resulting concentrations were averaged to derive a value equivalent to the measured fluorescence in the depicted area. The continuous decrease in fluorescence intensities due to bleaching of the dye was corrected using reference measurements with intact protoplasts. These cells were pre-loaded with fluorochrome and illuminated at the same laser intensity used in the diffusion experiments. The time course of the fluorescence signal was fitted by a single exponential decay to calculate the time constant for bleaching. Using the least squares method this corrected model fluorescence time course was then adopted to the measured data revealing the diffusion coefficients for the individual dye.

Parallel chlorophyll fluorescence and patch–clamp measurements

A MICROSCOPY-PAM Chlorophyll Fluorometer (Heinz Walz GmbH, Effeltrich, Germany) was combined with a patch–clamp set-up (Hamill *et al.*, 1981) in order to carry out chlorophyll fluorescence measurements and ion channel recordings on single *V. faba* guard cell protoplasts. After breaking the membrane under the patch-pipette and establishment of the whole-cell configuration ($t = 0.5$ min), dark–light induction curves were measured with repetitive application of saturation pulses to estimate the effective quantum yield of energy conversion at photosystem II reaction centres and the relative electron transport rate (Genty *et al.*, 1989; Schreiber *et al.*, 1994). K$^+$-channel activities in the plasma membrane of the same protoplast were determined right after recordings of the photosynthetic electron transport. Following the electrophysiological recordings, the measurements on the electron transport of the chloroplasts was repeated.

Chlorophyll fluorescence was measured as previously described (Goh *et al.*, 1999; Schreiber, 1998). This system is based on an epifluorescence microscope (Type Axiovert, Carl Zeiss GmbH, Oberkochen, Germany), with a single blue light (470 nm) emitting diode (LED) acting as source of modulated measuring light and a photomultiplier serving as fluorescence detector. The MICROSCOPY-PAM was operated in conjunction with a Pentium II PC and the WinControl-software (Walz). While actinic light intensity was 67 µmol m^{-2} sec^{-1} PAR, measuring light intensity was 0.8 µmol m^{-2} sec^{-1} and saturation pulse intensity amounted to 4280 µmol m^{-2} sec^{-1}, as measured with a special pin-hole micro-quantum-sensor (Walz).

Ion currents were recorded using an EPC-7 patch–clamp amplifier (HEKA, Lambrecht, Germany). Whole-cell data were low-pass filtered with an eight-pole Bessel filter at a cut-off frequency of

$$
\begin{aligned}
\frac{\Delta c(x, y, z)}{\Delta t} = {} & \left(\frac{D_{x+1,y,z} - D_{x-1,y,z}}{\Delta x}\right) \cdot \left(\frac{c_{x+1,y,z} - c_{x-1,y,z}}{2\Delta x}\right) \\
& + \left(\frac{D_{x+1,y,z} + D_{x-1,y,z}}{2}\right) \cdot \left(\frac{c_{x+1,y,z} - 2c_{x,y,z} + c_{x-1,y,z}}{\Delta x^2}\right) + \left(\frac{D_{x,y+1,z} - D_{x,y-1,z}}{\Delta y}\right) \cdot \left(\frac{c_{x,y+1,z} - c_{x,y-1,z}}{2\Delta y}\right) \\
& + \left(\frac{D_{x,y+1,z} + D_{x,y-1,z}}{2}\right) \cdot \left(\frac{c_{x,y+1,z} - 2c_{x,y,z} + c_{x,y-1,z}}{\Delta y^2}\right) + \left(\frac{D_{x,y,z+1} - D_{x,y,z-1}}{\Delta z}\right) \cdot \left(\frac{c_{x,y,z+1} - c_{x,y,z-1}}{2\Delta z}\right) \\
& + \left(\frac{D_{x,y,z+1} + D_{x,y,z-1}}{2}\right) \cdot \left(\frac{c_{x,y,z+1} - 2c_{x,y,z} + c_{x,y,z-1}}{\Delta z^2}\right)
\end{aligned}
\qquad (3)
$$

2 kHz. Data were sampled at 2.5 fold filter frequency, digitised (ITC-16, Instrutech Corp., Elmont, NY, USA), stored on hard disk and analysed with software of Instrutech Corp. on a Power-MacIntosh (Gravis TT200, Gravis GmbH, Berlin). Patch-pipettes were prepared from Kimax-51 glass (Kimble products, Vineland, NY, USA) and coated with silicone (Sylgard 184 silicone elastomer kit, Dow Corning, USA). In order to determine membrane potentials the command voltages were corrected off-line for liquid junction potentials according to Neher (Neher, 1992). The standard pipette solution (cytoplasm) contained 150 mM K-gluconate, 2 mM $MgCl_2$, 3 mM $CaCl_2$, 5 mM EGTA, ± 2 mM MgATP, 10 mM Hepes–Tris pH 7.4. The bathing medium contained 30 mM K-gluconate, 1 mM $CaCl_2$, 10 mM Mes–Tris pH 5.6. For measurements in the presence of ADP- and Pi-containing solutions, 2 mM MgATP were replaced by 2 mM K_2-ADP in addition to K_2HPO_4, and 2 mM $MgCl_2$ were added to give a final concentration of 4 mM Mg^{2+}. All solutions were adjusted to 400 mos mol kg^{-1} using D-sorbitol. Chemicals were obtained from Sigma (Sigma Chemie, Deisenhofen, Germany).

Acknowledgements

References

Bertl, A. and Felle, H. (1985) Cytoplasmic pH of root hair cells of *Sinapis alba* recorded by a pH-sensitive microelectrode: Does fusicoccin stimulate the proton pump by cytoplasmic acidification? *J. Exp. Bot.* **36**, 1142–1149.

Blatt, M.-R. (1988) Mechanisms of fusicoccin action: a dominant role for secondary transport in a higher-plant cell. *Planta*, **174**, 187–200.

Bölter, B., Soll, J., Hill, K., Hemmler, R. and Wagner, R. (1999) A rectifying ATP-regulated solute channel in the chloroplastic outer envelope from pea. *EMBO J.* **18**, 5505–5516.

Felle, H., Brummer, B., Bertl, A. and Parish, R.-W. (1986) IAA and fusicoccin cause cytosolic acidification of corn coleoptile cells. *Proc. Natl Acad. Sci. USA* **83**, 8992–8995.

Felle, H.H., Hanstein, S., Steinmeyer, R. and Hedrich, R. (2000) Dynamics of ionic activities in the apoplast of the sub-stomatal cavity of intact *Vicia faba* leaves during stomatal closure evoked by ABA and darkness. *Plant J.* **24**, 297–304.

Gautier, H., Vavasser, A., Gans, P. and Lasceve, G. (1991) Relationship between respiration and photosynthesis in guard cell and mesophyll cell protoplasts of Commelina communis L. *Plant Physiol.* **95**, 636–641.

Genty, B., Briantais, J.-M. and Baker, N.R. (1989) The relationship between the quantum yield of photosynthetic electron transport and quenching of chlorophyll fluorescence. *Biochim. Biophys. Acta* **990**, 87–92.

Goh, C.-H., Schreiber, U. and Hedrich, R. (1999) New approach of monitoring changes in chlorophyll a fluorescence of single guard cells and protoplasts in response to physiological stimuli. *Plant, Cell Environ.* **22**, 1057–1070.

Hamill, O.P., Marty, A., Neher, E., Sakmann, B. and Sigworth, F.J. (1981) Improved patch–clamp techniques for high-resolution current recording from cells and cell-free membrane patches. *Pflügers Arch.* **391**, 85–100.

Hoshi, T. (1995) Regulation of voltage dependence of the KAT1 channel by intracellular factors. *J. Gen. Physiol.* **105**, 309–328.

Klimov, V.V., Klevanik, A.V., Shuvalov, V.A. and Krasnovsky, A.A. (1977) Reduction of pheophytin in the primary light reaction of photosystem II. *FEBS Lett.* **82**, 183–186.

Li, J., Lee, Y.R. and Assmann, S.M. (1998) Guard cells possess a calcium-dependent protein kinase that phosphorylates the KAT1 potassium channel. *Plant Physiol.* **116**, 785–795.

Lohse, G. and Hedrich, R. (1992) Characterization of the plasma membrane proton ATPase from *Vicia faba* guard cells: Modulation by extracellular factors and seasonal changes. *Planta*, **188**, 206–214.

Mawson, B.-T. (1993) Modulation of photosynthesis and respiration in guard and mesophyll cell protoplasts by oxygen concentration. *Plant Cell Environ.* **16**, 207–214.

Michalke, B. and Schnabl, H. (1990) Modulation of the activity of phosphoenolpyruvate carboxylase during potassium-induced swelling of guard-cell protoplasts of *Vicia faba* L. after light and dark treatments. *Planta*, **180**, 188–193.

Mori, I.C. and Muto, S. (1997) Abscisic acid activates a 48-kD protein kinase in guard cell protoplasts. *Plant Physiol.* **113**, 833–839.

Müller-Röber, B., Ellenberg, J., Provart, N., Willmitzer, L., Busch, H., Becker, D., Dietrich, P., Hoth, S. and Hedrich, R. (1995) Cloning and electrophysiological analysis of KST1, an inward rectifying K^+-channel expressed in potato guard cells. *EMBO J.* **14**, 2409–2416.

Neher, E. (1992) Correction for liquid junction potentials in patch–clamp experiments. *Meth Enzymol.* **207**, 123–131.

Pusch, M. and Neher, E. (1988) Rates of diffusional exchange between small cells and a measuring patch pipette. *Pflügers Arch. Eur. J. Physiol.* **411**, 204–211.

Raschke, K. (1979) Movements of Stomata. In: *Encyclopedia of Plant Physiology, New Series, Physiology of Movements, 7 7* (Feinleib, H.W.A.M.E., ed.). New York: Springer Verlag, pp. 383–441.

Roelfsema, M.R.G., Steinmeyer, R., Staal, M. and Hedrich, R. (2001) Single guard cell recordings in intact plants: light-induced hyperpolarization of the plasma membrane. *Plant J.* **26**, 1–13.

Schreiber, U. (1998) Chlorophyll fluorescence: New instruments for special applications. In *Proceedings of the XIth International Congress on Photosynthesis*, Vol. V (Garab, G., ed.). Dordrecht: Kluwer Academic Publishers, pp. 4253–4258.

Schreiber, U., Bilger, W. and Neubauer, C. (1994) Chlorophyll fluorescence as a nonintrusive indicator for rapid assessment of *in vivo* photosynthesis. In *Ecophysiology of Photosynthesis: Ecological Studies* (Schulze E.-D. and Caldwell, M.M., eds). Berlin: Springer Press, pp. 49–70.

Schroeder, J.I. (1988) K^+ transport properties of K^+ channels in the plasma membrane of *Vicia faba* guard cells. *J. General Physiol.* **92**, 667–683.

Schroeder, J.I., Raschke, K. and Neher, E. (1987) Voltage dependence of potassium channels in guard-cell protoplasts. *Proc. Natl Acad. Sci. USA* **84**, 4108–4112.

Serrano, E.E., Zeiger, E. and Hagiwara, S. (1988) Red light stimulates an electrogenic proton pump in Vicia guard cell protoplasts. *Proc. Natl Acad. Sci. USA* **85**, 436–440.

Spalding, E.P. and Goldsmith, M.H.M. (1993) Activation of K+ channels in the plasma membrane of Arabidopsis by ATP produced photosynthetically. *Plant J.* **5**, 477–484.

Sze, H., Li, X. and Palmgren, M.G. (1999) Energization of plant cell membranes by H+-pumping ATPases: Regulation and biosynthesis. *Plant Cell* **11**, 677–689.

Szyroki, A., Ivashikina, N., Dietrich, P. *et al.* (2001) KAT1 is not essential for stomatal opening. *Proc. Natl Acad. Sci. USA* **98**, 2917–2921.

Tang, X.D. and Hoshi, T. (1999) Rundown of the hyperpolarization-activated KAT1 channel involves slowing of the opening transitions regulated by phosphorylation. *Biophys. J.* **76**, 3089–3098.

Wu, W.-H. and Assmann, S.-M. (1995) Is ATP required for K^+-channel activation in Vicia guard cells? *Plant Physiol.* **107**, 101–109.